SbcB facilitates natural transformation in *Vibrio cholerae* in an exonuclease-independent manner

Triana N. Dalia[1] and Ankur B. Dalia[1,*]

[1]Department of Biology, Indiana University, Bloomington, IN 47405.
*Correspondence to: ankdalia@iu.edu

ABTRACT
Natural transformation (NT) is a conserved mechanism of horizontal gene transfer in bacterial species. During this process, DNA is taken up into the cytoplasm where it can be integrated into the host genome by homologous recombination. We have previously shown that some cytoplasmic exonucleases can inhibit NT by degrading ingested DNA prior to its successful recombination. Here, however, we demonstrate that the exonuclease SbcB counterintuitively promotes NT in *Vibrio cholerae*. Through a systematic analysis of the distinct steps of NT, we show that SbcB acts downstream of DNA uptake into the cytoplasm, but upstream of recombinational branch migration. Through mutational analysis, we show that the SbcB promotes NT in a manner that does not rely on its exonuclease activity. Finally, we provide genetic evidence that SbcB directly interacts with the primary bacterial recombinase, RecA. Together, these data advance our molecular understanding of horizontal gene transfer in *V. cholerae*, and reveal that SbcB promotes homologous recombination during NT in a manner that does not rely on its canonical exonuclease activity.

IMPORTANCE
Horizontal gene transfer by natural transformation contributes to the spread of antibiotic resistance and virulence factors in bacterial species. Here, we study how one protein, SbcB, helps facilitate this process in the facultative bacterial pathogen *Vibrio cholerae*. SbcB is a well-known for its exonuclease activity (*i.e.*, the ability to degrade the ends of linear DNA). Through this study we uncover that while SbcB is important for natural transformation, it does not facilitate this process using its exonuclease activity. Thus, this work helps further our understanding of the molecular events required for this conserved evolutionary process, and uncovers a function for SbcB beyond its canonical exonuclease activity.

INTRODUCTION
Cells can acquire novel traits through horizontal gene transfer by natural transformation. During this process, cells take up free double-stranded DNA (dsDNA) from the environment. In Gram-negative bacteria, dsDNA is first taken up across the outer membrane via the combined action of dynamic DNA-binding type IV pili (1, 2) and the periplasmic DNA-binding molecular ratchet ComEA (3, 4). Then, a single strand of this DNA is translocated across the inner membrane by ComEC and ComF(C). Once this single-stranded DNA (ssDNA) is translocated into the cytoplasm, it can interact with proteins that help facilitate its integration into the host genome. This includes DprA, which protects ingested DNA and helps recruit RecA to initiate homologous recombination (5).

Because the tDNA that is imported into the cytoplasm is ssDNA, it is potentially sensitive to the action of ssDNA exonucleases that may act to degrade this DNA before it can be integrated into the genome. Indeed, we have previously found that deletion of the ssDNA exonucleases *recJ*

and *exoVII* enhances NT in *V. cholerae* (6). In particular, Δ*recJ* Δ*exoVII* mutants can be transformed at high rates with tDNA containing short arms of homology (6), which is consistent with these proteins normally degrading the ends of ssDNA tDNA in the cytoplasm to inhibit NT.

Contrary to this negative effect of the RecJ and ExoVII ssDNA exonucleases on NT, our prior results suggest that one ssDNA exonuclease, SbcB (also known as: exonuclease I, ExoI, and XonA), is required for optimal NT in *V. cholerae* (6). Here, we sought to determine the mechanism by which this exonuclease counterintuitively promotes NT.

RESULTS

SbcB is required for optimal NT

The genes required for NT in *V. cholerae* are tightly regulated and induced via two distinct regulatory inputs: chitin oligosaccharides and quorum sensing (7, 8). Our prior experiments assessed the impact of *sbcB* on NT in a strain background that is dependent on both of these regulatory inputs. Thus, one possibility is that SbcB is important for regulating the expression of genes required for NT. Regulatory control of NT can be bypassed by ectopically expressing the master regulator of competence TfoX and by constitutively activating quorum sensing via deletion of LuxO (1, 8, 9). So to test this hypothesis, we assessed the impact of *sbcB* on NT in a background where *tfoX* is ectopically expressed (P_{tac}-*tfoX*) and *luxO* is deleted. In this genetic background, we found that Δ*sbcB* exhibited a ~1.5-log decrease in NT (**Fig. 1**), which phenocopies what was previously observed when cells relied on natural induction via chitin and quorum sensing (6). This indicates that SbcB acts downstream of the regulatory steps that lead the expression of genes required for NT. All strains used throughout the remainder of the study contained P_{tac}-*tfoX* and Δ*luxO* mutations, which allowed us to bypass the need for chitin induction to study the effect of SbcB on NT.

SbcB does not facilitate the uptake of tDNA during NT

Next, we sought to identify the step of NT that is affected by SbcB. The first step of NT is the uptake of DNA from the environment, which requires the combined activities of dynamic DNA-binding competence type IV pili (T4P) to initiate the translocation of DNA across the outer membrane and a DNA-binding periplasmic molecular ratchet called ComEA. ComEA is a periplasmic dsDNA-binding protein, and it dynamically relocalizes upon DNA uptake, which can be monitored via functional fluorescent fusions like ComEA-mCherry (3, 4). The localization of ComEA-mCherry shifts from diffuse within the periplasm in the absence of tDNA uptake, to the formation of fluorescent foci when dsDNA is taken up into the periplasm (**Fig. 2A**). Thus, tracking the formation of ComEA-mCherry foci can allow for quantification of DNA uptake across the outer membrane. We assessed the formation of ComEA-mCherry foci after cells were incubated with tDNA for 30 mins (**Fig. 2A**). In the parent strain, almost all cells exhibited 1 or more ComEA-mCherry focus after this 30 min incubation (**Fig. 2B**). Consistent with tDNA uptake requiring T4P, mutating the critical T4P component PilQ (10, 11) prevents the formation of ComEA-mCherry foci (**Fig. 2B**). When we tested the *sbcB* mutant, we found that this strain could take up DNA into the periplasm in a manner that was indistinguishable from the parent (**Fig. 2B**; compare 30 min timepoints).

Following the uptake of dsDNA into the periplasm, a single strand of this tDNA is translocated across the inner membrane into the cytoplasm via the integral membrane protein ComEC (12, 13). And it is hypothesized that the strand of DNA that is not translocated into the cytoplasm is degraded. The molecular mechanism underlying the translocation of this single-stranded tDNA across the inner membrane remains very poorly understood. However, single cell tracking of the spatiotemporal dynamics of tDNA integration are consistent with the recombination of ssDNA

(14). Thus, we hypothesized that SbcB could be facilitating NT by promoting the degradation of one strand of tDNA to help translocate ssDNA into the cytoplasm. So, we next sought to test whether SbcB affects the translocation of tDNA into the cytoplasm.

In *V. cholerae*, the translocation of DNA across the outer and inner membranes is temporally uncoupled (15). Consistent with this, we find that the number of ComEA-mCherry foci in the Δ*comEC* strain following a 30 min incubation with tDNA is indistinguishable from the parent (**Fig. 2B**), indicating that the Δ*comEC* mutant still exhibits normal tDNA uptake into the periplasm. Because uptake across the two membranes is uncoupled, we hypothesized that the translocation of tDNA from the periplasm to the cytoplasm could be tracked indirectly using the same ComEA-mCherry reporter. Because as DNA is translocated across the inner membrane there should no longer be a DNA substrate for ComEA-mCherry to bind to in the periplasm, thus, resulting in the resolution of ComEA-mCherry foci (**Fig. 2A**). For this assay, it was critical to prevent cells from taking up any new tDNA, which would confound the ability to look at the resolution of ComEA-mCherry foci due to DNA translocation across the inner membrane. So after incubating cells with tDNA for 30 mins to allow for tDNA uptake into the periplasm, cells were treated with DNAse to prevent any additional tDNA uptake. Then, cells were incubated for 2 additional hours to allow for DNA translocation across the inner membrane. When we performed this experiment, we saw that the number of cells with ≥2 ComEA-mCherry foci was significantly reduced in the parent but not in the Δ*comEC* mutant. This is consistent with tDNA translocating across the inner membrane in the parent but not in the Δ*comEC* mutant, as expected. In this assay, the Δ*sbcB* mutant was indistinguishable from the parent, suggesting that SbcB does not facilitate the translocation of tDNA across the inner membrane.

SbcB does not facilitate branch migration during NT

Because SbcB was not required for the translocation of tDNA into the cytoplasm, we hypothesized that it was playing a role in the downstream process of tDNA integration. Our prior work demonstrates that following RecA-dependent strand invasion, the NT-specific helicase ComM facilitates branch migration of tDNA into the genome (16). An unusual property of ComM is that it exhibits bidirectional helicase activity and can translocate either 5'→3' or 3'→5' on DNA substrates *in vitro* (16). This bidirectional helicase activity, if stochastic, would be equally likely to promote or inhibit tDNA integration during NT. From experiments tracking the spatiotemporal dynamics of tDNA integration in single cells, however, it is clear that ComM promotes highly efficient homologous recombination during NT (14). This suggests that there may be additional factors *in vivo* that promote ComM directionality. Thus, we hypothesized that the exonuclease activity of SbcB may facilitate NT by regulating the directionality of ComM-dependent branch migration. Specifically, that SbcB degrades the genomic strand displaced by the integrating tDNA so that ComM branch migration can only proceed in one direction.

To test this, we used a previously established assay to assess branch migration activity *in vivo* (16). This assay detects branch migration indirectly via assessing the comigration of two linked genetic markers. Specifically, between a Trimethoprim resistance marker (Tm^R) and a nonsense mutation (*i.e.*, a premature stop codon) in *lacZ*, which we refer to as *lacZ** (**Fig. 3A**). We used two different tDNA products: one where Tm^R and *lacZ** are separated by 243 bp, and another where they are separated by 820 bp.

Cells are transformed with this linear tDNA and if branch migration is efficient, both markers are integrated into the genome. But if branch migration is inefficient, then cells may integrate the Tm^R marker (which is selected for in the experiment), but not the genetically linked *lacZ** mutation. When we assess the transformation frequency of the Tm^R marker in these experiments, we find that Δ*sbcB* and Δ*comM* are significantly attenuated compared to the

parent, which is consistent with SbcB and ComM both playing an important role during NT (**Fig. 3B**). When we assess the associated comigration (*i.e.*, the linkage with the *lacZ** mutation), we find that Δ*comM* is significantly reduced compared to the parent, which is consistent with the established role for ComM in branch migration during NT (**Fig. 3C**). However, the comigration of Δ*sbcB* is indistinguishable from the parent, despite the reduced transformation frequency in this background (**Fig. 3B-C**). This suggests that SbcB may not facilitate branch migration as hypothesized.

To further test this, we assessed the transformation frequency of a Δ*sbcB* Δ*comM* double mutant. If these proteins work together to promote branch migration, we would expect the transformation frequency of this double mutant to be similar to the single Δ*comM* or Δ*sbcB* mutant (*i.e.*, an epistasic interaction). But if these genes do not act together, then we would expect the transformation phenotype of Δ*sbcB* Δ*comM* to be the sum of the transformation deficits observed in each single mutant. When we performed this experiment using linear tDNA, we find that the reduction in NT in Δ*comM* Δ*sbcB* double mutant is the sum of the transformation defects observed in Δ*comM* and Δ*sbcB* single mutants (**Fig. 3D**). These results further suggest that SbcB and ComM act at distinct steps during NT. Thus, SbcB does not facilitate branch migration during NT.

SbcB acts upstream of ComM-dependent branch migration

Our data thus far show that SbcB acts downstream of DNA uptake into the cytoplasm. And that SbcB does not work with ComM to facilitate branch migration. To continue to narrow down where SbcB acts during NT, we next sought to determine whether SbcB acts upstream or downstream of ComM-dependent branch migration. We have previously demonstrated that a fluorescent translational fusion of ComM (GFP-ComM) dynamically forms foci in a manner that is dependent on RecA-mediated strand invasion (14). Thus, tracking the formation of GFP-ComM foci demarcates cells that are actively undergoing branch migration during NT (**Fig. 4A**). To test whether SbcB acted upstream of ComM-dependent branch migration, we assessed GFP-ComM focus formation in the parent and Δ*sbcB* by epifluorescence timelapse microscopy. We found that the percentage of cells that exhibited a GFP-ComM focus, and the number of GFP-ComM foci generated in those cells was significantly lower in the Δ*sbcB* mutant compared to the parent (**Fig. 4B-C**). These results suggest that SbcB is acting upstream of ComM-dependent branch migration.

SbcB is epistatic with RecA

Our data suggest that SbcB is acting downstream of DNA uptake into the cytoplasm and upstream of ComM-dependent branch migration. A prerequisite for ComM-dependent branch migration is RecA-mediated strand invasion (14). So next, we sought to determine whether SbcB facilitates RecA-mediated strand invasion. RecA is indispensable for homologous recombination. Thus, Δ*recA* is incapable of NT with linear tDNA that must integrate into the genome (10, 14).

Cells can also take up replicating plasmids by NT, and these products do not require homologous recombination into the host genome (16). As a result, recombination is dispensable when a replicating plasmid is used as tDNA. Consistent with this, Δ*comM* exhibits no reduction in NT with a replicating plasmid as tDNA compared to the parent (**Fig. 5**), which is in stark contrast to when linear tDNA that must recombine into the genome is used (**Fig. 3D**). Also, Δ*recA* is capable of NT with a replicating plasmid as tDNA, although this mutant does exhibit an ~10-fold reduction in NT (**Fig. 5**). DprA is an essential NT protein that protects ssDNA following translocation into the cytoplasm. Because DprA is critical for NT when a replicating plasmid is

used as tDNA, this suggests that cells are still taking up DNA via the same NT pathway in these experiments (**Fig. 5**).

Similar to Δ*recA*, we observed an ~10-fold reduction in NT in the Δ*sbcB* mutant. To determine if SbcB and RecA work together to promote NT, we assessed the phenotype of the Δ*sbcB* Δ*recA* double mutant. Interestingly, we found that these mutations were epistatic because the Δ*sbcB* Δ*recA* mutant has a phenotype that is statistically indistinguishable from the Δ*sbcB* single mutant (**Fig. 5**). If these proteins acted in completely separate pathways, the phenotype of the Δ*sbcB* Δ*recA* double mutant should be the sum of the NT defects observed in each single mutant (i.e., an ~2-log decrease in NT when compared to the parent). While it is not clear why RecA and SbcB are required for NT with a replicating plasmid tDNA (see **Discussion**), the observed epistasis suggests that RecA and SbcB are likely working in the same pathway to promote NT.

SbcB does not require its exonuclease activity to promote NT
SbcB is a DnaQ family exonuclease that has a highly conserved catalytic domain (17). To test whether the exonuclease activity of SbcB was required for its stimulatory effect on NT, we complemented Δ*sbcB* with an ectopic copy of *sbcB* containing mutations to two invariantly conserved residues within the catalytic site (*sbcB** = $sbcB^{D13AE15A}$). When we assessed NT, we were very surprised to find that *sbcB** did not phenocopy Δ*sbcB* (**Fig. 6A**). In fact, the NT frequency for Δ*sbcB lacZ*::*sbcB** was indistinguishable from the parent (**Fig. 6A**).

The catalytic residues of SbcB mutated to generate SbcB* are invariantly conserved among DnaQ family exonucleases (17), however, we sought to more rigorously test whether these mutations eliminate exonuclease activity. In *E. coli*, SbcB facilitates mismatch repair by participating in the excision reaction via its exonuclease activity. This is supported by the observation that 4 exonucleases, RecJ, ExoVII, ExoX, and SbcB, are redundant for mismatch repair in *E. coli* where the *recJ exoVII exoX sbcB* quadruple mutant has an ~6-fold elevated rate of acquiring spontaneous Rif^R mutations compared to the *recJ exoVII exoX* triple mutant (18). *V. cholerae* does not have a homolog of ExoX, but it does encode homologs to the ssDNA exonucleases RecJ, ExoVII and ExoIX. So first, we assessed whether SbcB facilitates mismatch repair in *V. cholerae*. To do this, we determined the spontaneous Rif^R mutation rate in a Δ*recJ* Δ*exoVII* Δ*exoIX* triple mutant vs a Δ*recJ* Δ*exoVII* Δ*exoIX* Δ*sbcB* quadruple mutant. We found that the latter strain exhibited a spontaneous Rif^R rate that was ~50-fold higher (**Fig. 6B**). However, the spontaneous Rif^R rate for the Δ*sbcB* single mutant was indistinguishable from the parent (**Fig. 6B**). This suggests that SbcB is redundant with other exonucleases for mismatch repair in *V. cholerae*, as previously observed in *E. coli* (18). This redundancy with other exonucleases also suggests that it is likely the exonuclease activity of SbcB that is required for mismatch repair. When we ectopically expressed *sbcB* vs *sbcB** in the Δ*recJ* Δ*exoVII* Δ*exoIX* Δ*sbcB* mutant, we found that the strain complemented with wildtype *sbcB* reduced the mutation rate to the level of *recJ exoVII exoX*, while the strain with *sbcB** was indistinguishable from the Δ*recJ* Δ*exoVII* Δ*exoIX* Δ*sbcB* parent (**Fig. 6B**). This strongly suggests that the mutations in SbcB* eliminate its exonuclease activity as hypothesized.

SbcB is narrowly conserved among gammaproteobacteria (19), and it has predominantly been studied and characterized in the model organism *Escherichia coli*. SbcB from *V. cholerae* is well-conserved to its *E. coli* homolog (59% identity, 74% similarity). To test whether *V. cholerae* SbcB has unique properties that allow it to facilitate NT, we complemented the Δ*sbcB* mutant by ectopically expressing *E. coli sbcB* ($sbcB_{Ec}$). We found that $SbcB_{Ec}$ could fully complement the Δ*sbcB* mutant as it restored NT back to parent levels (**Fig. 6A**). Furthermore, a catalytic mutant of $SbcB_{Ec}$ ($sbcB_{Ec}$* = $sbcB_{Ec}^{D15AE17A}$) also fully restored the NT of Δ*sbcB* back to parent levels

(**Fig. 6A**). All together, these results indicate that the exonuclease activity of SbcB is not required to facilitate NT, and that this is activity is not a unique property of *V. cholerae* SbcB.

SbcB interacts with RecA

Our data suggest that SbcB is likely facilitating RecA-dependent strand invasion in a manner that does not rely on its exonuclease activity. One possibility is that SbcB directly interacts with RecA to facilitate its activity. To test this, we performed Bacterial Adenylate Cyclase Two Hybrid (BACTH) assays (20) to assess the interaction between SbcB* and RecA. When we performed these assays, we found that SbcB* exhibited interactions with itself and RecA (**Fig. 7**). Because SbcB and RecA can both bind to ssDNA, this interaction may not reflect a direct interaction between these proteins, but could rather be an interaction that is bridged by a ssDNA substrate in the cell. To test this, we also performed BACTH analysis with DprA, which is also a ssDNA-binding protein (5). If ssDNA was helping to bridge interactions in our BACTH assays, we hypothesized that we should also observe interactions between SbcB* and DprA. However, when we tested this, no interactions were observed between SbcB* and DprA (**Fig. 7**). This suggests that the interactions observed between SbcB* and RecA are specific.

DISCUSSION

Our results demonstrate that SbcB acts downstream of tDNA uptake and upstream of ComM-dependent branch migration. Also, they show that the exonuclease activity of SbcB is dispensable for its role in promoting NT. These results help to narrow down the potential roles that SbcB plays during NT.

RecA assembly on ssDNA occurs unidirectionally from 5' → 3' (21). Thus, for RecA to bind to the 3' end of a long tDNA molecule, it must be processively assembled from an upstream 5' site. As a 3' → 5' exonuclease, SbcB binds to the 3' ends of ssDNA molecules. And our results suggest that SbcB directly interacts with RecA, which may help recruit RecA to the 3' end of single-stranded tDNA. There are at least two models that may explain why SbcB-dependent recruitment of RecA to the 3' end of tDNA promotes NT.

Our data demonstrate that SbcB is epistatic with RecA when a replicating plasmid is used as the tDNA. Because ssDNA is translocated into the cytoplasm during NT, cells must take up multiple independent complementary tDNA molecules to reassemble the plasmid into a replicative form. In the simplest case, cells would require the uptake of 2 tDNA molecules: one molecule that represents the entire ssDNA sequence of the plasmid, and a second partially complementary molecule that can prime synthesis of the other strand. While RecA-dependent strand invasion would not be necessary for this assembly, it is possible that RecA promotes annealing of complementary sequences, resulting in the observed 10-fold deficit for Δ*recA* when a replicating plasmid is used as tDNA. Furthermore, annealing of the 3' end of the complementary strand may be particularly important because this would allow for DNA replication to proceed, which is likely necessary to complete plasmid assembly. Thus, SbcB-dependent recruitment of RecA to the 3' end of tDNA molecules could help facilitate this activity. This is consistent with the observed epistasis between RecA and SbcB during plasmid transformation. When a linear tDNA homologous to the host chromosome is used, RecA loading on the 3' end could also facilitate homologous recombination by promoting strand invasion of the 3' end into the genome. This could allow the integrated 3' end to initiate DNA replication, which would stabilize the recombination intermediate (22). Interestingly, prior data suggest that SbcB facilitates RecA-dependent recombination *in vitro* (23). In these studies, however, it was presumed that this stimulatory effect of SbcB was due to its exonuclease activity.

A distinct possibility is that RecA contributes to the protection of single-stranded tDNA upon uptake into the cytoplasm. If so, the observed epistasis between SbcB and RecA is consistent with a model in which SbcB-dependent recruitment of RecA to 3' ends helps protect single-stranded tDNA in the cytoplasm from the action of other exonucleases. Prior work demonstrates that mutant alleles of SbcB with diminished exonuclease activity can protect 3' ends (24, 25). Also, single-stranded binding protein (SSB) directly interacts with SbcB to promote its exonuclease activity (26). During NT, tDNA is coated with DprA, which can evict SSB and promote the loading of RecA (5). So, SSB may be excluded from interacting with SbcB at the 3' end of the tDNA, which may hamper SbcB exonuclease activity during NT *in vivo*. Our observation that an exonuclease defective allele of SbcB is equally capable of promoting NT is consistent with this hypothesis.

All together, these results elucidate a novel role for the canonical exonuclease SbcB in facilitating the integration of tDNA during horizontal gene transfer by NT in *V. cholerae*. Future work will focus on testing whether SbcB-RecA interactions are required for SbcB to enhance NT. SbcB is narrowly conserved among gammaproteobacteria (19). But NT is broadly conserved in diverse microbial species (27). So it is tempting to speculate that the role that SbcB plays during NT in *V. cholerae*, is facilitated by other recombination proteins in more distantly related naturally transformable species.

METHODS

Bacterial Strains and Culture Conditions

All strains were derived from *V. cholerae* E7946 (28). Cells were routinely grown in LB Miller broth and agar supplemented with spectinomycin (200 µg/mL), kanamycin (50 µg/mL), trimethoprim (10 µg/mL), tetracycline (0.5 µg/mL), sulfamethoxazole (100 µg/mL), chloramphenicol (1 µg/mL), erythromycin (10 µg/mL), carbenicillin (20 µg/mL), or zeocin (100 µg/mL) as appropriate.

Construction of mutant strains

All strains were generated by natural transformation / MuGENT using splicing-by-overlap-extension (SOE) PCR mutant constructs exactly as previously described (29, 30). Ectopic expression constructs were generated by SOE PCR and integrated onto the *V. cholerae* genome exactly as previously described (31). All strains were confirmed by PCR and/or sequencing. For a detailed list of all mutants used in this study, see **Table S1.** For a complete list of primers used to generate mutant constructs, see **Table S2**.

Natural transformation assays

As discussed in the text, cells were engineered to bypass the native signals required for NT in *V. cholerae*. Specifically, the master competence regulator TfoX was overexpressed via an isopropyl β-d-1-thiogalactopyranoside (IPTG)-inducible P_{tac} promoter, and the cells are genetically locked in a high cell density state via deletion of *luxO*, as previously described . Chitin-independent transformation assays to determine NT frequency were performed exactly as previously described (1). Briefly, cells were grow at 30ºC rolling in LB supplemented with 100 µM IPTG, 20 mM $MgCl_2$, 10 mM $CaCl_2$ to late-log. Then, ~10^8 CFUs were diluted into instant ocean medium (7g/L; Aquarium Systems). Next, transforming DNA (tDNA) was added into each reaction as appropriate. For linear tDNA that must integrate into the genome, 100 ng of a ΔVC1807::Erm^R product was used. VC1807 is a frame-shifted transposase gene. For replicating plasmid as tDNA, pBAD18-Kan (32) was miniprepped from *E. coli* TG1. Control reactions were performed for each strain where no tDNA was added. Cells were incubated with tDNA overnight. Then, reactions were outgrown by adding 1mL of LB and shaking at 37ºC for 3 hours.

Reactions were then plated for quantitative culture by dribble plating on LB agar supplemented with the appropriate antibiotic to quantify transformants, and plain LB to quantify total viable counts. Transformation frequency is defined as the CFU/mL of transformants divided by the CFU/mL of total viable counts.

For assays where branch migration was indirectly assessed via linkage analysis, transformation reactions were performed exactly as described above except that they were plated onto LB agar supplemented with trimethoprim and X-gal (40 µg/mL). On these plates, all cells integrated the Tm^R marker, and if cells integrated the genetically linked *lacZ* nonsense mutation they would make white colonies. If they did not integrate the linked lacZ nonsense mutation, they would make blue colonies on these plates. Thus, the comigration frequency is defined as the percent of Tm^R colonies that were white on these plates.

Spontaneous Rif^R mutant frequency assays
All strains were isolation streak plated onto plain LB agar. Then, single colonies were picked and grown overnight in plain LB. These cultures were then concentrated and ~10^{10} CFUs were spread onto LB agar plates supplemented with Rifampicin 100 µg/mL to quantify Rif^R mutants. Concentrated cultures were also dilution dribble plated onto plain LB agar plates to quantify total CFU. The Rif^R mutant frequency is defined as Rif^R CFU / total CFU.

Microscopy
Phase contrast and fluorescence images were collected on a Nikon Ti-2 microscope using a Plan Apo × 60 objective, a YFP and/or mCherry filter cube, a Hamamatsu ORCA Flash 4.0 camera and Nikon NIS Elements imaging software.

To assess ComEA-mCherry localization upon DNA uptake, cells were grown to induce competence as described above for natural transformation assays. Then, ~10^7 cells were mixed with ~750 ng of a 6kb PCR product as tDNA. Reactions were incubated at 30ºC static for 30 mins to allow for tDNA uptake into the periplasm. Half the reaction was then placed on ice for imaging at this time point. DNAse was added to the other half of the reaction, which was then incubated at 37ºC for 120 mins. Then, both samples (30 min and 150 min) were placed under 0.2% gelzan pads and imaged. The number of ComEA-mCherry foci was determined by analyzing 60 cells per replicate.

To assess GFP-ComM focus formation, cells were grown to induce competence as described above for natural transformation assays. Then, ~10^7 cells were mixed with ~650 ng of a 6kb tDNA product that will integrate into the genome, and placed under an 0.2% gelzan pad. Samples were then subjected to timelapse imaging where images were taken every 2 min for 3 hours. The number of GFP-ComM foci was determined by analyzing 60 cells per replicate.

Bacterial Adenylate Cyclase Two-Hybrid (BACTH) Assays
Gene inserts were amplified by PCR and cloned into the pUT18C, pUT18, pKT25, or pKNT25 vectors to generate N- and C- terminal fusions to the T18 and T25 fragments of adenylate cyclase. Miniprepped vectors were then cotransformed into *E. coli* BTH101 and outgrown with 500 µL LB for 1 hour at 37°C with shaking. Reactions were plated on LB agar plates supplemented with kanamycin 50 µg/mL and carbenicillin 100 µg/mL to select for transformants that received both plasmids. Single colonies were then picked and grown statically at 30°C in LB supplemented with kanamycin 50 µg/mL and carbenicillin 100 µg/mL. Then, 3 µL of each strain was spotted onto LB agar plates supplemented with kanamycin 50 µg/mL, carbenicillin 100µg/mL, 0.5 mM IPTG and 40 µg/mL X-gal. Plates were incubated at 30°C for 24 hours prior to imaging on an Epson Perfection V600 scanner.

Statistics
Statistical differences were assessed using GraphPad Prism software. The statical tests employed are indicated in figure legends. Descriptive statistics for all samples, and a comprehensive list of statistical comparisons can be found in **Dataset S1**.

ACKNOWLEDGEMENTS
This work was supported by grant R35GM128674 from the National Institutes of Health to ABD.

REFERENCES

1. Ellison CK, Dalia TN, Vidal Ceballos A, Wang JC, Biais N, Brun YV, Dalia AB. 2018. Retraction of DNA-bound type IV competence pili initiates DNA uptake during natural transformation in Vibrio cholerae. Nat Microbiol 3:773-780.
2. Dubnau D, Blokesch M. 2019. Mechanisms of DNA Uptake by Naturally Competent Bacteria. Annu Rev Genet 53:217-237.
3. Gangel H, Hepp C, Muller S, Oldewurtel ER, Aas FE, Koomey M, Maier B. 2014. Concerted spatio-temporal dynamics of imported DNA and ComE DNA uptake protein during gonococcal transformation. PLoS Pathog 10:e1004043.
4. Seitz P, Pezeshgi Modarres H, Borgeaud S, Bulushev RD, Steinbock LJ, Radenovic A, Dal Peraro M, Blokesch M. 2014. ComEA is essential for the transfer of external DNA into the periplasm in naturally transformable Vibrio cholerae cells. PLoS Genet 10:e1004066.
5. Mortier-Barriere I, Velten M, Dupaigne P, Mirouze N, Pietrement O, McGovern S, Fichant G, Martin B, Noirot P, Le Cam E, Polard P, Claverys JP. 2007. A key presynaptic role in transformation for a widespread bacterial protein: DprA conveys incoming ssDNA to RecA. Cell 130:824-36.
6. Dalia TN, Yoon SH, Galli E, Barre FX, Waters CM, Dalia AB. 2017. Enhancing multiplex genome editing by natural transformation (MuGENT) via inactivation of ssDNA exonucleases. Nucleic Acids Res 45:7527-7537.
7. Meibom KL, Blokesch M, Dolganov NA, Wu CY, Schoolnik GK. 2005. Chitin induces natural competence in Vibrio cholerae. Science 310:1824-7.
8. Lo Scrudato M, Blokesch M. 2012. The regulatory network of natural competence and transformation of Vibrio cholerae. PLoS Genet 8:e1002778.
9. Bassler BL, Wright M, Silverman MR. 1994. Sequence and function of LuxO, a negative regulator of luminescence in Vibrio harveyi. Mol Microbiol 12:403-12.
10. Seitz P, Blokesch M. 2013. DNA-uptake machinery of naturally competent Vibrio cholerae. Proc Natl Acad Sci U S A 110:17987-92.
11. Weaver SJ, Ortega DR, Sazinsky MH, Dalia TN, Dalia AB, Jensen GJ. 2020. CryoEM structure of the type IVa pilus secretin required for natural competence in Vibrio cholerae. Nat Commun 11:5080.
12. Lacks S. 1962. Molecular fate of DNA in genetic transformation of Pneumococcus. J Mol Biol 5:119-31.
13. Inamine GS, Dubnau D. 1995. ComEA, a Bacillus subtilis integral membrane protein required for genetic transformation, is needed for both DNA binding and transport. J Bacteriol 177:3045-51.
14. Dalia AB, Dalia TN. 2019. Spatiotemporal Analysis of DNA Integration during Natural Transformation Reveals a Mode of Nongenetic Inheritance in Bacteria. Cell 179:1499-1511 e10.

15. Seitz P, Blokesch M. 2014. DNA transport across the outer and inner membranes of naturally transformable Vibrio cholerae is spatially but not temporally coupled. MBio 5:e01409-14.
16. Nero TM, Dalia TN, Wang JC, Kysela DT, Bochman ML, Dalia AB. 2018. ComM is a hexameric helicase that promotes branch migration during natural transformation in diverse Gram-negative species. Nucleic Acids Res 46:6099-6111.
17. Fijalkowska IJ, Schaaper RM. 1996. Mutants in the Exo I motif of Escherichia coli dnaQ: defective proofreading and inviability due to error catastrophe. Proc Natl Acad Sci U S A 93:2856-61.
18. Viswanathan M, Burdett V, Baitinger C, Modrich P, Lovett ST. 2001. Redundant exonuclease involvement in Escherichia coli methyl-directed mismatch repair. J Biol Chem 276:31053-8.
19. Lovett ST. 2011. The DNA Exonucleases of Escherichia coli. EcoSal Plus 4.
20. Karimova G, Pidoux J, Ullmann A, Ladant D. 1998. A bacterial two-hybrid system based on a reconstituted signal transduction pathway. Proc Natl Acad Sci U S A 95:5752-6.
21. Cox MM, Lehman IR. 1981. Directionality and polarity in recA protein-promoted branch migration. Proc Natl Acad Sci U S A 78:6018-22.
22. Gupta RC, Golub EI, Wold MS, Radding CM. 1998. Polarity of DNA strand exchange promoted by recombination proteins of the RecA family. Proc Natl Acad Sci U S A 95:9843-8.
23. Konforti BB, Davis RW. 1992. ATP hydrolysis and the displaced strand are two factors that determine the polarity of RecA-promoted DNA strand exchange. J Mol Biol 227:38-53.
24. Thoms B, Borchers I, Wackernagel W. 2008. Effects of single-strand DNases ExoI, RecJ, ExoVII, and SbcCD on homologous recombination of recBCD+ strains of Escherichia coli and roles of SbcB15 and XonA2 ExoI mutant enzymes. J Bacteriol 190:179-92.
25. Razavy H, Szigety SK, Rosenberg SM. 1996. Evidence for both 3' and 5' single-strand DNA ends in intermediates in chi-stimulated recombination in vivo. Genetics 142:333-9.
26. Lu D, Myers AR, George NP, Keck JL. 2011. Mechanism of Exonuclease I stimulation by the single-stranded DNA-binding protein. Nucleic Acids Res 39:6536-45.
27. Lorenz MG, Wackernagel W. 1994. Bacterial gene transfer by natural genetic transformation in the environment. Microbiol Rev 58:563-602.
28. Miller VL, DiRita VJ, Mekalanos JJ. 1989. Identification of toxS, a regulatory gene whose product enhances toxR-mediated activation of the cholera toxin promoter. J Bacteriol 171:1288-93.
29. Dalia AB. 2018. Natural Cotransformation and Multiplex Genome Editing by Natural Transformation (MuGENT) of Vibrio cholerae. Methods Mol Biol 1839:53-64.
30. Dalia AB, McDonough E, Camilli A. 2014. Multiplex genome editing by natural transformation. Proc Natl Acad Sci U S A 111:8937-42.
31. Dalia TN, Chlebek JL, Dalia AB. 2020. A modular chromosomally integrated toolkit for ectopic gene expression in Vibrio cholerae. Sci Rep 10:15398.
32. Guzman LM, Belin D, Carson MJ, Beckwith J. 1995. Tight regulation, modulation, and high-level expression by vectors containing the arabinose PBAD promoter. J Bacteriol 177:4121-30.

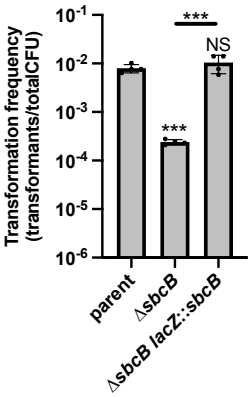

Fig. 1. **SbcB facilitates NT in *Vibrio cholerae.*** Natural transformation assays of the indicated strains. Data are from four independent biological replicates and shown as the mean ± SD. Statistical comparisons were made by one-way ANOVA with Tukey's multiple comparison test of the log-transformed data. NS, not significant. *** = $p < 0.001$

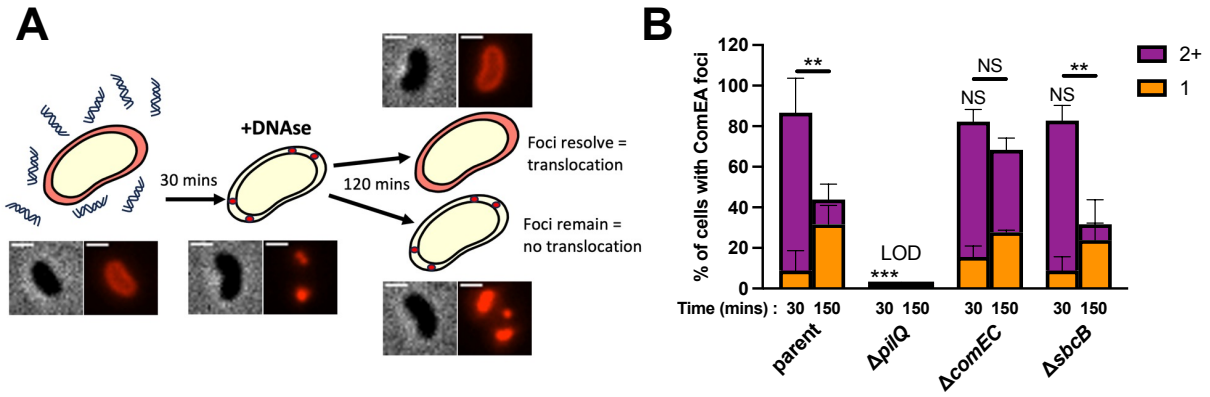

Fig. 2. **SbcB does not affect DNA uptake during NT.** (**A**) Schematic and representative images of the experimental setup used to assess DNA uptake during NT. Cells contained a ComEA-mCherry fusion and were incubated with tDNA. The presence of a ComEA-mCherry focus indicates that tDNA is taken up into the periplasm. After 30 mins, DNAse was added to remove all extracellular DNA. The subsequent tracking of ComEA-mCherry foci was used as an indirect readout to demarcate the translocation of periplasmic tDNA into the cytoplasm. Scale bar, 1 µm. (**B**) The assay described in **A** was performed in the indicated strain backgrounds and the frequency of cells with 1 or more than 1 (2+) ComEA-mCherry foci is reported at the indicated time points. Data are from 3 independent biological replicates and shown as the mean ± SD; n = 180 cells analyzed in each strain background. Statistical comparisons for the frequencies of cells with 2+ ComEA-mCherry foci were made by one-way ANOVA with Tukey's multiple comparison test of the log-transformed data. LOD, limit of detection. NS, not significant. ** = $p < 0.01$

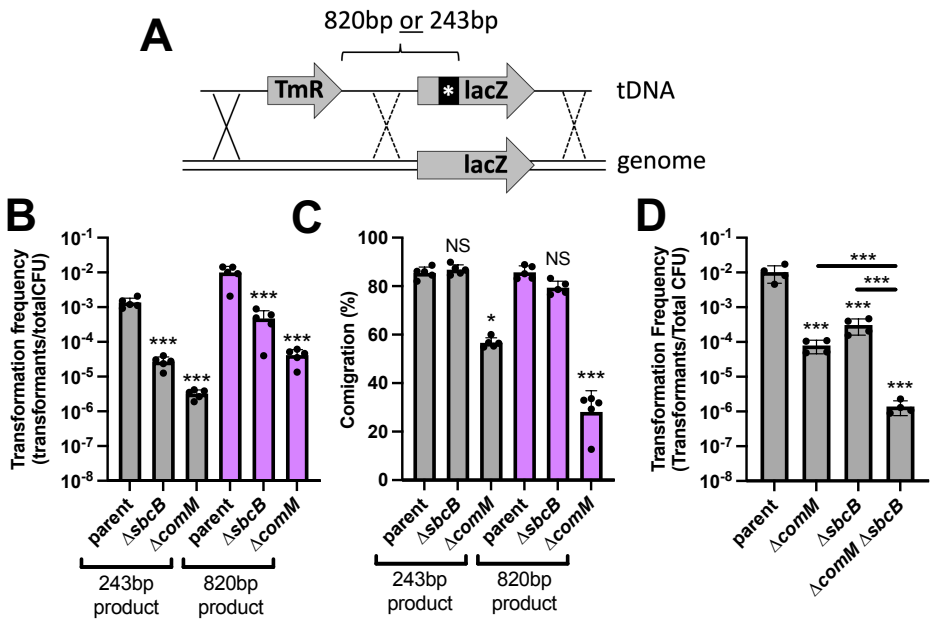

Fig. 3. **SbcB does not promote ComM-dependent branch migration.** (**A**) Schematic of the experimental setup to assess branch migration via linkage analysis between a trimethoprim resistance marker (Tm^R) and a nonsense mutation in *lacZ*. Two different tDNAs were used: one where the *lacZ* nonsense mutation was 243 bp away from the Tm^R cassette, and another where the spacing was 820 bp. The two tDNA products described in **A** were naturally transformed into the indicated strains and the (**B**) transformation frequency and (**C**) comigration frequency (i.e., the frequency of linkage between the Tm^R and *lacZ* nonsense mutation) are reported. All strains in these assays contained a Δ*mutS* mutation to prevent mismatch repair from confounding the results. (**D**) Natural transformation assays of the indicated strains. All data are from at least 4 independent biological replicates and shown as the mean ± SD. Statistical comparisons were made by one-way ANOVA with Tukey's multiple comparison test of the log-transformed data. NS, not significant. *** = $p < 0.001$, ** = $p < 0.01$, * = $p < 0.05$. Statistical identifiers directly above bars represent comparisons to the parent.

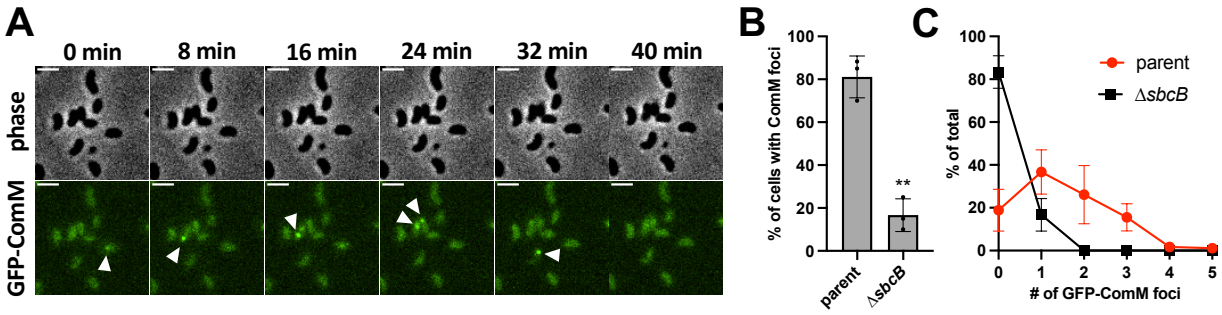

Fig. 4. **SbcB acts upstream of ComM-dependent branch migration.** (**A**) Montage of timelapse imaging of cells expressing a GFP-ComM fluorescent fusion incubated with tDNA. White arrows indicate the appearance of transient GFP-ComM foci. Scale bar, 2 µm. Experiments were performed as in **A** in the parent and Δ*sbcB* background to quantify the (**B**) proportion of cells that exhibited any GFP-ComM foci and the (**C**) distribution of the GFP-ComM foci observed. Data are from 3 independent biological replicates and shown as the mean ± SD; n = 180 cells analyzed in each strain background. Statistical comparison in **B** was made by unpaired Student's t-test of the log-transformed data. ** = $p < 0.01$. Statistical identifier directly above bar represents comparisons to the parent.

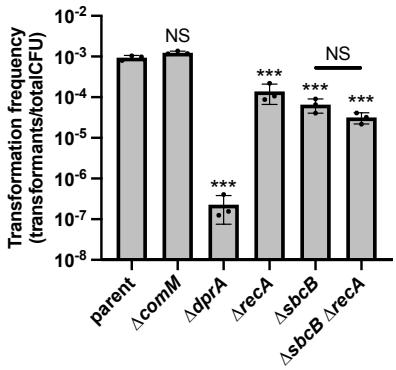

Fig. 5. **SbcB is epistatic with RecA during NT when a replicating plasmid is used as the tDNA.** Natural transformation assays of the indicated strains using a replicating plasmid as the tDNA. Data are from at least 3 independent biological replicate and shown as the mean ± SD. Statistical comparisons were made by one-way ANOVA with Tukey's multiple comparison test of the log-transformed data for each tDNA product. NS, not significant. *** = $p < 0.001$. Statistical identifiers directly above bars represent comparisons to the parent.

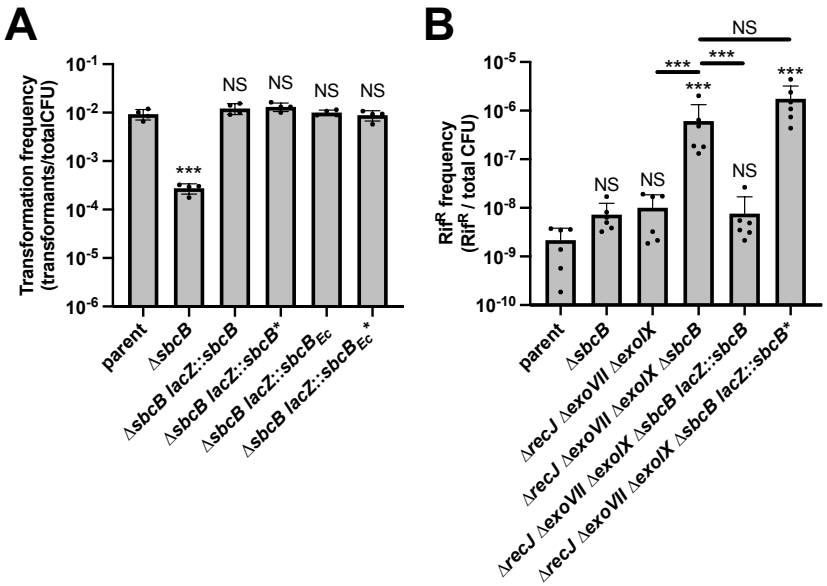

Fig. 6. **SbcB facilitates NT in *Vibrio cholerae* independent of its exonuclease activity.** (**A**) Natural transformation assays of the indicated strains using linear tDNA. (**B**) Quantifying the frequency of spontaneous Rif^R mutants in the indicated strain backgrounds. All data are from at least 4 independent biological replicates and shown as the mean ± SD. NS, not significant. *** = $p < 0.001$. Statistical identifiers directly above bars represent comparisons to the parent.

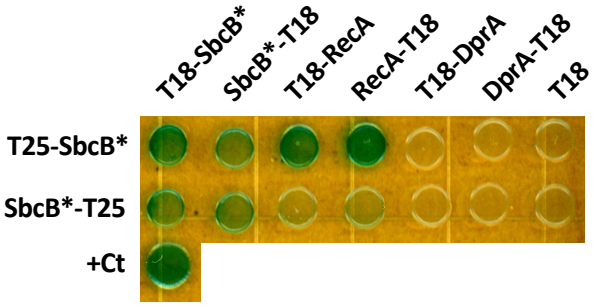

Fig. 7. **SbcB interacts with RecA.** Bacterial Adenylate Cyclase Two-Hybrid (BACTH) assays were performed to assess pairwise interactions between SbcB* (SbcB* = the $SbcB^{D13A,E15A}$ catalytic mutant) and RecA or DprA. The indicated proteins were fused to the T18 or T25 fragments of adenylate cyclase as indicated. Leucine zipper fusions to T18 and T25 served as a positive control for interacting proteins (+Ct). Data are representative of 3 independent biological replicates.

Table S1 - *Strains used in this study*

Strain #*	Genotype	Figures	Use in manuscript
SAD030	*V. cholerae* E7946 Sm^R	Fig. 6B	parent for all strains in this study, and the parent for spontaneous Rif^R mutant frequency assays
TND0905 / SAD2468	P_{tac}-*tfoX*, Δ*luxO, lacZ*::*lacI*^{q}, *pilA*^{S67C}, Δ*VC1807*::*Zeo*^{R}	Fig. 1, 3D, 5, 6A	parent for NT frequency assays
TND4174 / SAD3565	Δ*sbcB*::*Tm*^{R}, P_{tac}-*tfoX*, Δ*luxO, lacZ*::*lacI*^{q}, *pilA*^{S67C}, Δ*VC1807*::*Zeo*^{R}	Fig. 1, 3D, 5, 6A	Δ*sbcB* for NT frequency assays
TND4301 / SAD3566	Δ*lacZ*::*Spec*^{R}-P_{native}-*sbcB*, Δ*sbcB*::*Tm*^{R}, P_{tac}-*tfoX*, Δ*luxO*, *pilA*^{S67C}, Δ*VC1807*::*Zeo*^{R}	Fig. 1, 6A	Δ*sbcB lacZ*::*sbcB* for NT frequency assays
TND2245 / SAD3567	Δ*comM*::*Carb*^{R}, P_{tac}-*tfoX*, Δ*luxO, lacZ*::*lacI*^{q}, *pilA*^{S67C}, Δ*VC1807*::*Zeo*^{R}	Fig. 3D, 5	Δ*comM* for NT frequency assays
TND4175 / SAD3568	Δ*sbcB*::*Tm*^{R}, Δ*comM*::*Carb*^{R}, P_{tac}-*tfoX*, Δ*luxO, lacZ*::*lacI*^{q}, *pilA*^{S67C}, Δ*VC1807*::*Zeo*^{R}	Fig. 3D	Δ*sbcB* Δ*comM* for NT frequency assays
TND1072 / SAD3569	Δ*dprA*::*Cm*^{R}, P_{tac}-*tfoX*, Δ*luxO, lacZ*::*lacI*^{q}, *pilA*^{S67C}, Δ*VC1807*::*Zeo*^{R}	Fig. 5	Δ*dprA* for NT frequency assays
TND4543 / SAD3570	Δ*recA*::*Spec*^{R}, P_{tac}-*tfoX*, Δ*luxO, lacZ*::*lacI*^{q}, *pilA*^{S67C}, Δ*VC1807*::*Zeo*^{R}	Fig. 5	Δ*recA* for NT frequency assays
TND4542 / SAD3571	Δ*recA*::*Spec*^{R}, Δ*sbcB*::*Tm*^{R}, Δ*comM*::*Carb*^{R}, P_{tac}-*tfoX*, Δ*luxO, lacZ*::*lacI*^{q}, *pilA*^{S67C}, Δ*VC1807*::*Zeo*^{R}	Fig. 5	Δ*sbcB* Δ*recA* for NT frequency assays
TND4338 / SAD3572	Δ*lacZ*::*Spec*^{R}-P_{native}-*sbcB*^{D13A,E15A}, Δ*sbcB*::*Tm*^{R}, P_{tac}-*tfoX*, Δ*luxO*, *pilA*^{S67C}, Δ*VC1807*::*Zeo*^{R}	Fig. 6A	Δ*sbcB lacZ*::*sbcB** for NT frequency assays
TND4407 / SAD3573	Δ*lacZ*::*Spec*^{R}-P_{native}-*sbcB*$_{E.coli}$, Δ*sbcB*::*Tm*^{R}, P_{tac}-*tfoX*, Δ*luxO*, *pilA*^{S67C}, Δ*VC1807*::*Zeo*^{R}	Fig. 6A	Δ*sbcB lacZ*::*sbcB*$_{Ec}$ for NT frequency assays
TND4472 / SAD3574	Δ*lacZ*::*Spec*^{R}-P_{native}-*sbcB*$_{E.coli}^{D15A,D17A}$, Δ*sbcB*::*Tm*^{R}, P_{tac}-*tfoX*, Δ*luxO*, *pilA*^{S67C}, Δ*VC1807*::*Zeo*^{R}	Fig. 6A	Δ*sbcB lacZ*::*sbcB*$_{Ec}$* for NT frequency assays
TND0111 / SAD1505	Δ*sbcB*::*Kan*^{R}	Fig. 6B	Δ*sbcB* for spontaneous Rif^R mutant frequency assays
TND4599 / SAD3575	Δ*recJ*::*Zeo*^{R}, Δ*exoVII*::*Carb*^{R}, Δ*exoIX*::Kan^R	Fig. 6B	Δ*recJ* Δ*exoVII* Δ*exoIX* for spontaneous Rif^R mutant frequency assays
TND4605 / SAD3576	Δ*sbcB*::*Tm*^{R}, Δ*recJ*::*Zeo*^{R}, Δ*exoVII*::*Carb*^{R}, Δ*exoIX*::Kan^R	Fig. 6B	Δ*sbcB* Δ*recJ* Δ*exoVII* Δ*exoIX* for spontaneous Rif^R mutant frequency assays
TND4606 / SAD3577	Δ*lacZ*::*Spec*^{R}-P_{native}-*sbcB*, Δ*sbcB*::*Tm*^{R}, Δ*recJ*::*Zeo*^{R}, Δ*exoVII*::*Carb*^{R}, Δ*exoIX*::Kan^R	Fig. 6B	Δ*sbcB* Δ*recJ* Δ*exoVII* Δ*exoIX lacZ*::*sbcB* for spontaneous Rif^R mutant frequency assays
TND4607 / SAD3578	Δ*lacZ*::*Spec*^{R}-P_{native}-*sbcB*^{D13A,E15A}, Δ*sbcB*::*Tm*^{R}, Δ*recJ*::*Zeo*^{R}, Δ*exoVII*::*Carb*^{R}, Δ*exoIX*::Kan^R	Fig. 6B	Δ*sbcB* Δ*recJ* Δ*exoVII* Δ*exoIX lacZ*::*sbcB** for spontaneous Rif^R mutant frequency assays
TND0904 / SAD2436	*comEA-mCherry*, P_{tac}-*tfoX*, Δ*luxO, lacZ*::*lacI*^{q}, *pilA*^{S67C}, Δ*VC1807*::*Cm*^{R}	Fig. 2	parent for ComEA-mCherry localization assays
TND4170 / SAD3579	Δ*pilQ*::*Tet*^{R}, *comEA-mCherry*, P_{tac}-*tfoX*, Δ*luxO, lacZ*::*lacI*^{q}, *pilA*^{S67C}, Δ*VC1807*::*Cm*^{R}	Fig. 2	Δ*pilQ* for ComEA-mCherry localization assays
JLC645 / SAD3580	Δ*comEC*::*Kan*^{R}, *comEA-mCherry*, P_{tac}-*tfoX*, Δ*luxO, lacZ*::*lacI*^{q}, *pilA*^{S67C}, Δ*VC1807*::*Cm*^{R}	Fig. 2	Δ*comEC* for ComEA-mCherry localization assays
TND4173 / SAD3581	Δ*sbcB*::*Tm*^{R}, *comEA-mCherry*, P_{tac}-*tfoX*, Δ*luxO, lacZ*::*lacI*^{q}, *pilA*^{S67C}, Δ*VC1807*::*Cm*^{R}	Fig. 2	Δ*sbcB* for ComEA-mCherry localization assays

SAD1063	*Kan^R-Ptac-tfoX, ΔmutS*	Fig. 3B-C	parent for *in vivo* branch migration assays
TND2585 / SAD3582	*ΔsbcB::Spec^R, Kan^R-Ptac-tfoX, ΔmutS*	Fig. 3B-C	Δ*sbcB* for *in vivo* branch migration assays
SAD1071	*ΔcomM::Spec^R, Kan^R-Ptac-tfoX, ΔmutS*	Fig. 3B-C	Δ*comM* for *in vivo* branch migration assays
TND1474 / SAD3583	*ΔlacZ::P$_{lac}$-CFP-parB$_{P1}$-mCherry-parB$_{MT1}$ Zeo^R, 0.11Mbp::parS$_{MT1}$, GFP-comM, P$_{tac}$-tfoX, ΔluxO, pilA^{S67C}, ΔVC1807::Cm^R*	Fig. 4A-C	parent for GFP-ComM localization assays
TND1509 / SAD3584	*ΔsbcB::Tm^R, ΔlacZ::P$_{lac}$-CFP-parB$_{P1}$-mCherry-parB$_{MT1}$ Zeo^R, 0.11Mbp::parS$_{MT1}$, GFP-comM, P$_{tac}$-tfoX, ΔluxO, pilA^{S67C}, ΔVC1807::Cm^R*	Fig. 4B-C	Δ*sbcB* for GFP-ComM localization assays
SAD3547	*E. coli* TG1, pKT25-*sbcB^{D13A,E15A}*	Fig. 7	Harbors theT25-SbcB* vector for BACTH analysis
SAD3549	*E. coli* TG1, pKNT25-*sbcB^{D13A,E15A}*	Fig. 7	Harbors the SbcB*-T25 vector for BACTH analysis
SAD3558	*E. coli* TG1, pUT18C-*sbcB^{D13A,E15A}*	Fig. 7	Harbors the T18-SbcB* vector for BACTH analysis
SAD3551	*E. coli* TG1, pUT18-*sbcB^{D13A,E15A}*	Fig. 7	Harbors the SbcB*-T18 vector for BACTH analysis
TMN0416 / SAD3585	*E. coli* TG1, pUT18C-*recA*	Fig. 7	Harbors the T18-RecA vector for BACTH analysis
TMN0419 / SAD3587	*E. coli* TG1, pUT18-*recA*	Fig. 7	Harbors the RecA-T18 vector for BACTH analysis
TMN0417 / SAD3586	*E. coli* TG1, pUT18C-*dprA*	Fig. 7	Harbors the T18-DprA vector for BACTH analysis
TMN0420 / SAD3588	*E. coli* TG1, pUT18-*dprA*	Fig. 7	Harbors the DprA-T18 vector for BACTH analysis
SAD2240	*E. coli* TG1, pUT18C	Fig. 7	Harbors the T18 empty vector for BACTH analysis
SAD2241	*E. coli* TG1, pUT18C-zip	Fig. 7	Harbors the T18-zip vector for BACTH analysis
SAD2238	*E. coli* TG1, pKT25-zip	Fig. 7	Harbors the T25-zip vector for BACTH analysis

*Multiple Strain# designations indicate that the strain was stocked in two independent strain collections.

Table S2 – *Primers used in this study*

Primer*	Sequence (5' → 3')	Description
BBC688	TGGATGAGTGCTAAATGATGC	Δ*sbcB* (*i.e.*, ΔVC1234) F1
BBC689	gtcgacggatccccggaatCATGTGGCTTACCAAATCGC	Δ*sbcB* (*i.e.*, ΔVC1234) R1
BBC690	gaagcagctccagcctacaTGCTAACATCGTTTATTTTTACTTGC	Δ*sbcB* (*i.e.*, ΔVC1234) F2
BBC691	AACATGGTAAACAGCACCATC	Δ*sbcB* (*i.e.*, ΔVC1234) R2
DOG0582	ACATCTGGCAGATCTGATTTCAC	Δ*pilQ* (*i.e.*, ΔV2630) F1
DOG0583	gtcgacggatccccggaatCAACCGATTATTTTAAAGCCAGCTTG	Δ*pilQ* (*i.e.*, ΔV2630) R1
DOG0584	gaagcagctccagcctacaTAACTTAGCGTGTGCGTAACAAG	Δ*pilQ* (*i.e.*, ΔV2630) F2
DOG0585	TTGTGTTTGCTCTAACGTTTGC	Δ*pilQ* (*i.e.*, ΔV2630) R2
BBC411	CAAGATTGGCAATGGAGCGAC	Δ*comEC* (*i.e.*, ΔVC1879) F1
BBC412	gtcgacggatccccggaatCATAATCCCGTATGCCAAGAAAATTC	Δ*comEC* (*i.e.*, ΔVC1879) R1
BBC546	gaagcagctccagcctacaATGACCGATACTCAGTCTAACC	Δ*comEC* (*i.e.*, ΔVC1879) F2
BBC414	TCATCCATGCTCATGCTGCG	Δ*comEC* (*i.e.*, ΔVC1879) R2
ABD820	CGCTCTTATCTGCTTGGATAATGG	Δ*dprA* (*i.e.*, ΔVC0048) F1
ABD998	gtcgacggatccccggaatCATTAACTGGCATCATCAACC	Δ*dprA* (*i.e.*, ΔVC0048) R1
ABD999	gaagcagctccagcctacaTAGCTATGATGATGGATATTTTGATG	Δ*dprA* (*i.e.*, ΔVC0048) F2
ABD996	GGTTTGGTTATCCGGATCACAC	Δ*dprA* (*i.e.*, ΔVC0048) R2
ABD855	CATGAATCACTTTGGCATGAGG	Δ*comM* (*i.e.*, ΔVC0032) F1
ABD856	gtcgacggatccccggaatCATTGCTTCCCTTAGTATTTGATC	Δ*comM* (*i.e.*, ΔVC0032) R2
ABD857	gaagcagctccagcctacaTAGTACTCTGACCTGCAGAGTTC	Δ*comM* (*i.e.*, ΔVC0032) F2
ABD858	AAATTCCAGAAAAACCACGTC	Δ*comM* (*i.e.*, ΔVC0032) R2
BBC678	TGGATGCCAATCAACATTCG	Δ*recJ* (*i.e.*, ΔVC2417) F1
BBC679	gtcgacggatccccggaatCATACTGTGACAGGCCAAAG	Δ*recJ* (*i.e.*, ΔVC2417) R1
BBC680	gaagcagctccagcctacaGAAGCGAAATGATTGAAAACAACG	Δ*recJ* (*i.e.*, ΔVC2417) F2
BBC681	GATCGCATCCACAATGTTAGC	Δ*recJ* (*i.e.*, ΔVC2417) R2
DOG0185	TTCACTTCACCCAGTACACGC	Δ*exoVII* (*i.e.*, ΔVC0766) F1
DOG0186	gtcgacggatccccggaatCAACGCTGATTCCTCAGACG	Δ*exoVII* (*i.e.*, ΔVC0766) R1
DOG0187	gaagcagctccagcctacaTTAATGGATGGTGAGATTCTCTC	Δ*exoVII* (*i.e.*, ΔVC0766) F2
DOG0188	AGTTTGTAGAGGTTGTTATGGTAC	Δ*exoVII* (*i.e.*, ΔVC0766) R2
DOG0190	AGAAGAACTCTGTTTTGCATTAGAAC	Δ*exoIX* (*i.e.*, ΔVC0898) F1
DOG0191	gtcgacggatccccggaatCAAGCGACGAGTTCATGCTTG	Δ*exoIX* (*i.e.*, ΔVC0898) R1
DOG0192	gaagcagctccagcctacaTAAATCCCCTCTGATTAGCATC	Δ*exoIX* (*i.e.*, ΔVC0898) F2
DOG0193	TTAACCCTGACGTGACCGTG	Δ*exoIX* (*i.e.*, ΔVC0898) R2
BBC5040	CAAGTagCGTAcgCGAAAAAGAAGAATGTGGGCTGGTGTTCTTGCT	$sbcB^{D13AE15A}$ R1
BBC5041	TTCTTTTTCGcgTACGctACTTGGGGAGTCAATCCCGCAAAAGATC	$sbcB^{D13AE15A}$ F2

BBC4977	gcctggagtgcctaatgagGCTGAACAAATAATGGGATAGC	Amplify *sbcB* to clone at an ectopic locus with its native promoter intact F
BBC3101	tgtaggctggagctgcttcTTAGCAAGCGAGTTTTTCCACG	Amplify *sbcB* to clone at an ectopic locus with its native promoter intact R
BBC5065	tttagcgatttggtaagccacATGATGAATGACGGTAAGCAAC	Amplify *E. coli* sbcB to clone at an ectopic locus F
BBC5066	tgtaggctggagctgcttcTTAGACAATCTCTTCCGCGTAC	Amplify *E. coli* sbcB to clone at an ectopic locus R
BBC5145	AGGTagCGTAcgCGTGAAACAAAAAGGTAGATTGTTGCTTACCGTC	*E. coli sbcB*^{D15AE17A} R1
BBC5146	TTGTTTCACGcgTACGctACCTTTGGCACGCACCCCGCGTTAGATC	*E. coli sbcB*^{D15AE17A} F2
BBC5195	gcaggtggagcaggtggaCAGCAAGAACACCAGCCCAC	Amplify *sbcB** for TXX-*sbcB** or *sbcB**-TXX for BACTH F
BBC3103	tgtaggctggagctgcttcTTAGGCTGCGATTAATAGCTCTTTAG	Amplify *sbcB** for TXX-*sbcB** for BACTH R
BBC5196	tccaccacttccacctgcGCAAGCGAGTTTTTCCACGTAATGG	Amplify *sbcB** for *sbcB**-TXX for BACTH R
TMN0198	gcaggtggagcaggtggaGACGAGAATAAACAGAAGGCAC	Amplify *recA* for TXX-*recA* or *recA*-TXX for BACTH F
TMN0199	tgtaggctggagctgcttcTTAAAACTCTTCTGGCACCGC	Amplify *recA* for TXX-*recA* for BACTH R
TMN0200	tccaccacttccacctgcAAACTCTTCTGGCACCGC	Amplify *recA* for *recA*-TXX for BACTH R
TMN0210	gcaggtggagcaggtggaAAAGATCAGGATTTAGCGGCATG	Amplify *dprA* for TXX-*dprA* or *dprA*-TXX for BACTH F
TMN0211	tgtaggctggagctgcttcCTAGCCTCTCCCCTTTCTAATATAGC	Amplify *dprA* for TXX-*dprA* for BACTH R
TMN0212	tccaccacttccacctgcGCCTCTCCCCTTTCTAATATAGCC	Amplify *dprA* for *dprA*-TXX for BACTH R

*Lower case nucleotides on the 5’ end demarcate overlap sequences for SOE PCR. While internal lower case nucleotides demarcate point mutations.